

Identification and Characterization of Pectenotoxin (PTX) 4 and PTX7 as Spiroketal Stereoisomers of Two Previously Reported Pectenotoxins

Katsunori Sasaki, Jeffrey L. C. Wright, and Takeshi Yasumoto*

Faculty of Agriculture, Tohoku University, Tsutsumidori-Amamiya, Aoba-ku, Sendai 981, Japan;
Institute for Marine Biosciences, National Research Council of Canada, 1411 Oxford Street, Halifax,
Nova Scotia, Canada B3H 3Z1

Received July 17, 1997 (Revised Manuscript Received December 3, 1997)

Pectenotoxins (PTXs) isolated from the scallop *Patinopecten yessoensis* were shown to be involved in an episode of diarrhetic shellfish poisoning (DSP). A total of eight analogues (PTX1–PTX7 and PTX10) have been isolated to date, and the structures of four of these analogues (PTX1, PTX2, PTX3, and PTX6) have already been elucidated. Here, we report the characterization of PTX4 and PTX7 as 7-*epi*-PTX1 and 7-*epi*-PTX6, respectively, on the basis of NMR data and an acid-catalyzed chemical interconversion. The structures of two new artifacts, PTX8 and PTX9, produced following this treatment are also reported.

Introduction

The pectenotoxins (PTXs) (Figure 1) are a family of cyclic polyether macrolide toxins that have been found in the digestive glands of toxic scallops^{1–4} together with okadaic acid (OA) and dinophysistoxin-1 (DTX1), the principal toxins of the diarrhetic shellfish poisoning (DSP).⁴ PTX2 (**2**) induces diarrhea and liver damage.⁵ Whereas OA and its analogues are powerful phosphatase inhibitors,^{4,6} the PTXs do not possess this activity, and their mode of action still remains to be determined. Nevertheless, the poisoning associated with these toxins, and possibly others, is spread worldwide, posing a serious threat to public health and to the aquaculture industry.¹

To date, a total of eight PTX analogues (PTX1–PTX7 and PTX10) have been isolated from toxic extracts of the scallop *Patinopecten yessoensis*.^{1–4} Five of these (PTX1–PTX5) were obtained from neutral fractions of an Al₂O₃ column separation, and three others (PTX6, PTX7, and PTX10) were found in acidic fractions.³ The compound PTX1 (**1**) was the first of the pectenotoxin family to be characterized, and its structure was secured by X-ray crystallography (Figure 1).¹ Later, the structures of three other analogues **2**, **3**, and **6** (PTX2, PTX3, and PTX6) were determined by spectroscopic methods and comparison with **1**.^{1–3} The combined data indicated that the structural variation between these analogues resides in the nature of the substituent at C-18, where all stages of oxidation from methyl to carboxyl are found: PTX2: CH₃, PTX1: CH₂OH, PTX3: CHO, and PTX6: COOH (Figure 1).⁴ Recently, the absolute configuration of PTX6

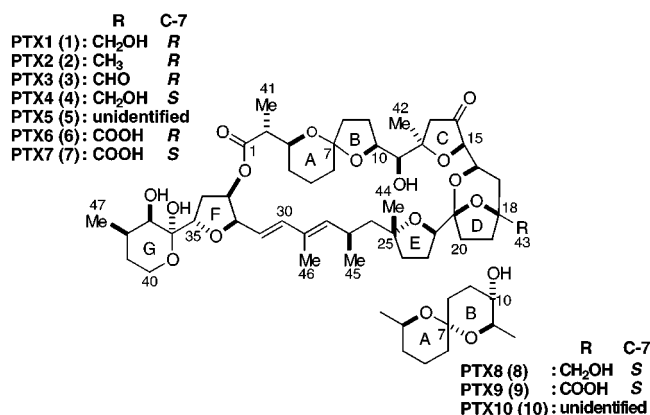


Figure 1. The structures of pectenotoxins (PTXs). To avoid the interconversion arising from the presence of a carboxyl group at C-43, all NMR measurements of the PTX6 (**6**), PTX7 (**7**), and PTX9 (**9**) congeners were carried out using the corresponding phenacyl ester derivative.

has been determined by NMR spectroscopy using phenylglycine methyl ester (PGME) as a chiral anisotropic reagent.⁷ As is often the case with families of shellfish toxins, the compounds are not produced by the shellfish themselves, but rather are products of toxigenic microalgae or phytoplankton ingested by the shellfish. Various dinoflagellate species of the genera *Dinophysis* and *Prorocentrum* are known to produce a variety of polyether toxins.^{3,4,8} Strains of the dinoflagellate *Dinophysis fortii* which produce OA and/or DTX1 were also found to produce PTX2 (**2**) in Japan⁹ and Europe.¹⁰ Interestingly, **2** was the only PTX congener found in both studies, leading to the proposal that **2** is the parent toxin which

(1) Yasumoto, T.; Murata, M.; Oshima, Y.; Sano, M.; Matsumoto, G. K.; Clardy, J. *Tetrahedron* **1985**, *41*, 1019.

(2) Murata, M.; Sano, M.; Iwashita, T.; Naoki, H.; Yasumoto, T. *Agric. Biol. Chem.* **1986**, *50*, 2693.

(3) Yasumoto, T.; Murata, M.; Lee, J.-S.; Torigoe, K. in *Bioactive Molecules: Mycotoxins and Phycotoxins '88*; Natori, S., Hashimoto, K., Ueno, Y., Eds.; Elsevier: New York, 1989; Vol 10, p 375.

(4) Yasumoto, T.; Murata, M. *Chem. Rev.* **1993**, *93*, 1897.

(5) Ishige, M.; Satoh, N.; Yasumoto, T. *Reps. Hokkaido Inst. Health*, **1988**, *38*, 15.

(6) (a) Takai, A.; Bialojan, C.; Troschka M.; Rüegg, J. C. *FEBS Lett.* **1987**, *217*, 81. (b) Cohen, P.; Holmes, C. F. B.; Tsukitani, Y. *Trends Biochem. Sci.* **1990**, *15*, 98.

(7) Sasaki, K.; Satake, M.; Yasumoto, T. *Biosci. Biotech. Biochem.* **1997**, *61*, 1783.

(8) (a) Shimizu, Y. *Chem. Rev.* **1993**, *93*, 1685. (b) Garson, M. J. *ibid.* 1699.

(9) Lee, J.-S.; Igarashi, T.; Fraga, S.; Dahl, E.; Hovgaard, P.; Yasumoto, T. *J. Appl. Phycol.* **1989**, *1*, 147.

(10) Draisci, R.; Lucentini, L.; Gianetti, L.; Boria, P.; Poletti, R. *Toxicol.* **1996**, *34*, 923.

Table 1. ^1H and ^{13}C Chemical Shifts of the Phenacyl Esters of PTX6, PTX7, and PTX9^a

position	PTX6			PTX7			PTX9		
	^1H	$^1\text{H}'$	^{13}C	^1H	$^1\text{H}'$	^{13}C	^1H	$^1\text{H}'$	^{13}C
1			172.6			173.1			170.7
2	2.61		48.6	2.68		47.8	2.84		45.7
2-Me(41)	1.27		15.1	1.30		16.1	1.11		14.2
3	3.58		76.2	3.97		72.5	3.65		73.4
4	1.24(ax)	1.60(eq)	29.9	1.43(ax)	1.92(eq)	29.5	1.33(ax)	1.66(eq)	26.0
5	1.35(ax)	1.60(eq)	22.0	1.92(ax)	1.55(eq)	20.6	1.69(ax)	1.49(eq)	19.6
6	1.78(ax)	1.62(eq)	34.4	1.67(ax)	1.79(eq)	33.7	1.41(ax)	1.53(eq)	34.9
7			107.5			106.2			96.6
8	1.32	2.20	32.6	2.10	2.16	39.8	1.51(ax)	1.84(eq)	34.7
9	1.49	2.09	22.3	2.31	2.72	25.4	2.30(ax)	1.99(eq)	27.6
10	4.35		81.1	4.92		79.7	3.99		67.4
10-OH	—			—			4.61		
11	4.39		74.9	4.28		77.6	3.82		79.2
11-OH	4.22			6.72			—		
12			81.8			82.3			83.6
12-Me(42)	1.23		23.1	1.50		22.4	1.40		19.9
13	2.17	3.33	44.5	2.48	3.12	49.3	2.65	2.78	51.6
14			213.7			213.5			212.0
15	4.06		79.2	4.13		80.3	4.14		79.8
16	4.60		70.6	4.54		70.2	4.48		70.4
17	3.06(ax)	2.01(eq)	33.1	3.11(ax)	2.01(eq)	33.3	3.04(ax)	2.01(eq)	32.6
18			82.5			82.8			82.7
19	2.25	2.56	31.5	2.29	2.59	31.7	2.27	2.59	31.7
20	1.95	2.48	27.5	2.04	2.41	29.6	1.88	2.49	27.3
21			110.3			109.8			110.5
22	4.37		79.2	4.25		79.9	4.24		78.8
23	1.85	2.33	29.8	1.95	2.01	28.5	1.73	1.94	30.2
24	1.41	1.58	37.3	1.47	1.54	37.8	1.28	1.64	35.5
25			84.5			84.1			84.8
25-Me(44)	1.21		26.6	1.32		26.8	1.14		26.7
26	1.57	1.75	50.6	1.42	1.57	49.5	1.55	1.69	50.4
27	2.49		30.4	2.64		30.0	2.43		30.2
27-Me(45)	0.92		23.6	0.92		23.5	0.92		23.6
28	5.09		140.2	5.06		140.3	5.09		139.6
29			130.5			130.8			130.8
29-Me(46)	1.59		12.5	1.70		12.7	1.67		13.0
30	6.69		135.0	6.63		134.6	6.63		134.5
31	5.50		121.7	5.56		122.1	5.51		123.0
32	4.98		83.1	4.97		82.9	4.94		82.8
33	5.78		75.2	5.75		75.8	5.66		75.4
34	2.57	2.72	34.1	2.60	2.70	34.1	2.60	2.68	34.1
35	5.30		82.7	5.20		82.5	5.28		82.7
36			98.6			98.6			98.6
36-OH	7.09			7.04			7.06		
37	3.86		71.2	3.82		71.0	3.84		71.1
37-OH	5.96			5.91			5.95		
38	2.54		30.2	2.52		30.3	2.54		30.2
38-Me(47)	1.15		18.2	1.15		18.2	1.18		18.3
39	1.99(ax)	1.26(eq)	28.0	1.97(ax)	1.25(eq)	28.1	2.02(ax)	1.29(eq)	28.1
40	4.30(aq)	3.84(eq)	60.9	4.28(aq)	3.82(eq)	60.9	4.29(ax)	3.86(eq)	60.9
43			171.4			171.4			171.3

^a ^1H NMR chemical shifts measured in pyridine-*d*₅ (ref δ 7.211). ^{13}C NMR chemical shifts measured in pyridine-*d*₅ (ref δ 123.5).

is metabolized in scallops to yield the congeners **1**, **3**, and **6**.³

Although the structure and origin of PTX toxins **1–3** and **6** can be accounted for in this way, the situation with the remaining four congeners, PTX4, PTX5, PTX7, and PTX10, is more complex, and their structures have not been determined as yet, primarily due to the small amounts of the compounds currently available. However, as the structural information of all the toxic constituents found in the scallops is essential for designing proper analytical methods and for understanding toxin metabolism in shellfish, we renewed our effort to isolate and determine the structures of these uncharacterized analogues. In this paper we report the structural elucidation of PTX4 (**4**) and PTX7 (**7**), as well as the isolation and characterization of two new artifacts, PTX8 (**8**) and PTX9 (**9**).

Results

The PTX6/7 pair of congeners shared a common molecular ion in FABMS [m/z 887 ($M - H$)⁻], as did the PTX1/4 pair [m/z 875 ($M + H$)⁺]. In addition, the LSI-MS/MS spectra of the ($M + \text{Na}$)⁺ ion for PTX6 (**6**) and PTX7 (**7**) were essentially identical, and a similar result was observed for the MS/MS fragmentation spectra of the ($M + \text{Na}$)⁺ ion of PTX1 (**1**) and PTX4 (**4**). Thus the MS data indicated that PTX6 and PTX7 are isomeric, as are PTX1 and PTX4. However, inspection of the NMR data further extended the relationship between the two pairs. The ^1H and ^{13}C NMR data for the PTX6/7 congeners and PTX1/4 congeners are shown in Table 1 and Table 2, respectively. Upon comparison of the data for PTX7 (**7**) with that for PTX4 (**4**), and similarly from previous comparisons between PTX6 (**6**) with PTX1 (**1**),³ it was clear in each case that these pairs of molecules

Table 2. ^1H and ^{13}C Chemical Shifts of PTX1, PTX4, and PTX8^a

position	PTX1			PTX4			PTX8		
	^1H	$^1\text{H}'$	^{13}C	^1H	$^1\text{H}'$	^{13}C	^1H	$^1\text{H}'$	^{13}C
1			172.6			173.1			170.7
2	2.63		48.6	2.68		47.8	2.83		45.8
2-Me(41)	1.30		15.2	1.30		16.2	1.08		14.2
3	3.58		76.2	3.98		72.5	3.63		73.4
4	1.22(ax)	1.61(eq)	29.9	1.42(ax)	1.90(eq)	29.4	1.30(ax)	1.63(eq)	26.1
5	1.34(ax)	1.65(eq)	22.0	1.92(ax)	1.54(eq)	20.6	1.69(ax)	1.48(eq)	19.6
6	1.78(ax)	1.60(eq)	34.4	1.67(ax)	1.80(eq)	33.7	1.38(ax)	1.53(eq)	34.9
7			107.5			106.3			96.5
8	1.29	2.19	32.6	2.08	2.18	39.8	1.48(ax)	1.81(eq)	34.6
9	1.47	2.13	22.3	2.33	2.77	25.5	2.30(ax)	1.98(eq)	27.5
10	4.33		81.0	4.94		79.8	3.97		67.4
11	4.39		75.1	4.25		77.6	3.79		79.2
12			81.7			82.1			83.5
12-Me(42)	1.22		23.2	1.48		22.6	1.36		20.0
13	2.16	3.34	44.5	2.45	3.12	49.2	2.64	2.73	51.7
14			213.8			213.7			212.1
15	4.07		79.7	4.12		80.9	4.10		80.4
16	4.53		71.1	4.46		70.8	4.34		70.9
17	2.78(ax)	1.46(eq)	32.1	2.80(ax)	1.46(eq)	32.5	2.71(ax)	1.44(eq)	31.6
18			84.0			84.2			84.2
19	1.78	2.12	29.3	1.81	2.12	29.4	1.78	2.11	29.4
20	1.93	2.43	27.9	2.01	2.35	30.1	1.86	2.40	27.8
21			109.6			109.1			109.7
22	4.35		79.6	4.22		80.1	4.20		79.2
23	1.86	2.37	29.8	1.93	2.05	28.6	1.72	1.93	30.3
24	1.42	1.61	37.4	1.49	1.52	37.5	1.28	1.63	35.5
25			84.2			83.9			84.5
25-Me(44)	1.22		26.7	1.31		26.9	1.10		26.8
26	1.64	1.81	50.9	1.50	1.64	49.7	1.59	1.73	50.6
27	2.51		30.4	2.63		30.1	2.44		30.2
27-Me(45)	0.93		23.6	0.92		23.5	0.91		23.6
28	5.09		140.2	5.10		140.3	5.11		139.6
29			130.5			130.8			130.8
29-Me(46)	1.60		12.5	1.70		12.6	1.67		13.0
30	6.69		135.1	6.65		134.9	6.64		134.9
31	5.50		121.7	5.55		122.1	5.50		123.1
32	4.97		83.0	4.97		82.9	4.92		82.8
33	5.79		75.1	5.77		75.7	5.66		75.4
34	2.57	2.73	34.1	2.58	2.72	34.1	2.58	2.68	34.1
35	5.31		82.6	5.21		82.5	5.28		82.7
36			98.6			98.6			98.6
37	3.86		71.1	3.83		71.0	3.85		71.1
38	2.56		30.2	2.53		30.2	2.54		30.2
38-Me(47)	1.15		18.3	1.14		18.3	1.15		18.3
39	2.00(ax)	1.27(eq)	28.0	1.97(ax)	1.25(eq)	28.0	2.02(ax)	1.25(eq)	28.1
40	4.31(aq)	3.86(eq)	60.9	4.28(aq)	3.82(eq)	60.9	4.28(ax)	3.83(eq)	60.9
43	3.85	3.93	67.3	3.85	3.93	67.3	3.83	3.91	67.1

^a ^1H NMR chemical shifts measured in pyridine-*d*₅ (ref δ 7.211). ^{13}C NMR chemical shifts measured in pyridine-*d*₅ (ref δ 123.5). OH signals were not observed because H₂O signal was irradiated.

shared a common carbon skeleton, differing only in the nature of the substituent at C-18: In **4** (and **1**) it is hydroxymethyl, while in **7** (and **6**) it is carboxyl,³ leading to the conclusion that **4** and **7** are stereoisomers of **1** and **6**, respectively.

Acid-Catalyzed Interconversion of the PTXs. Upon standing in aqueous acetonitrile solution, PTX7 (**7**) underwent gradual transformation to PTX6 (**6**) whereas PTX4 (**4**) remained unchanged under the same conditions. Since **7** contains a carboxyl group and **4** does not, it was suspected that the rearrangement was acid catalyzed. Indeed, addition of TFA (0.1% v/v) to an aqueous acetonitrile solution of **7** not only accelerated the conversion of **7** to **6**, but also resulted in formation of an additional isomeric product coded PTX9 (**9**) (Figures 1 and 2). In addition, **6**, which is stable during the purification and isolation process, also underwent equilibration to **7** and **9** following similar treatment with TFA (Figures 1 and 2). The proportions of isomers at equilibration (after 48 h) were PTX6:PTX7:PTX9 (40:16:44).

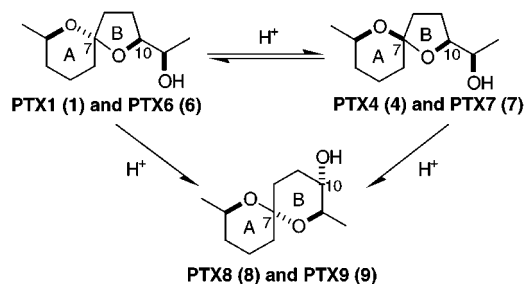


Figure 2. Acid-catalyzed Interconversion of the PTXs.

Under the same acid conditions, a similar equilibration was induced between the previously stable derivatives PTX1 (**1**) and PTX4 (**4**), together with formation of a new compound PTX8 (**8**) (Figure 2). Thus treatment of **1** with TFA yielded the equilibrium mixture of PTX1:PTX4:PTX8 (29:14:57). As further evidence for the role of acid in the rearrangement process, the phenacyl ester of PTX7 (**7**), which is normally stable upon standing under neutral

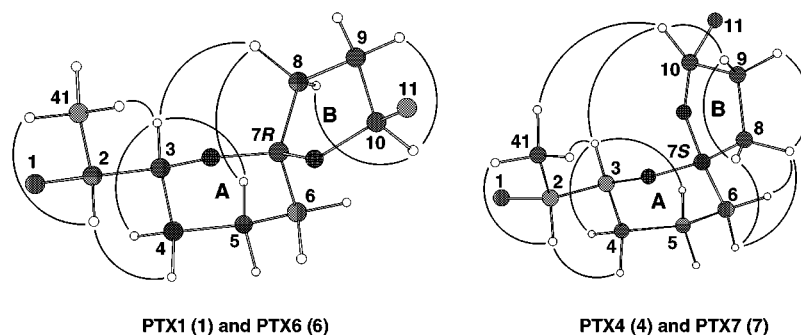


Figure 3. Equivalent portions of the PTX1/6 and PTX4/7 molecules, showing the NOEs around the spiroketal rings A and B.

conditions and does not undergo spontaneous rearrangement, rapidly gave the equilibration mixture PTX6 ester:PTX7 ester:PTX9 ester (30:9:61) following exposure to TFA.

The Structure of PTX7 (7). To avoid any interconversion catalyzed by the C-18 carboxyl group, all NMR measurements of the PTX6 and PTX7 congeners were carried out using the corresponding phenacyl ester derivatives. As a prelude to the structural assignment of the phenacyl ester of PTX7, it was necessary to completely assign the ^1H and ^{13}C signals for the phenacyl ester of the characterized PTX6 isomer using conventional 2D NMR experiments. These data were then used in the assignment of the PTX7 resonances and the data for both compounds are shown in Table 1. On the basis of the NMR connectivity data it was concluded that PTX7 (7) possessed the same planar structure as PTX6 (6). For example, the ^1H - ^1H COSY spectra for 7 and 6 both displayed similar patterns of cross-peaks, although some differences in chemical shifts were observed. The connectivities around the quaternary carbons established by the HMBC data were also identical between compounds though the single correlation H-9/C-7 observed in 6 was absent in the HMBC spectrum of 7. In the latter case, C-7 was assigned by default as the last remaining unassigned spiroketal carbon. Further careful comparison of the NMR data of 6 and 7 revealed a series of ^1H chemical shift differences (in the range Δ 0.2–0.7 ppm) between the corresponding protons H-3 to H-13 in the region around rings A–C. The most significant differences were observed for H-3, and H-8 through H-10, though smaller differences were also observed for H-22, H-23, H-26, and H-27. In each isomer, the corresponding carbons in the region C-3 through C-15 also displayed chemical shift differences, some quite significant (e.g. C-3, C-8, C-9, C-11, and C-13), whereas there was little difference in the ^{13}C resonances for carbons in the region C-22 through C-27. Together, these data suggested that the structural difference between the two isomers was in the region around rings A and B which form a spiro-[4.5] system. Since it is known that acid treatment of spiroketal systems can lead to epimerization at the spiroketal carbon,¹¹ it was suspected that acid-catalyzed ring opening and reclosure of this system might lead to epimerization at C-7. Such a stereochemical change in this region of the PTX molecule would be expected to result in conformational changes to the entire macrocyclic lactone ring and would explain the minor chemical shift

differences observed for a few other resonances elsewhere in the molecule (e.g. H-22, H-23, H-26, and H-27).

In PTX6 (6) and PTX7 (7), coupling patterns of H-3 (ddd, 11, 11, and 2 Hz), were similar and consistent with their axial configuration, indicating that the conformation of the tetrahydropyran ring A in PTX7 (7) is not flipped. From previous studies and based on the X-ray crystallographic data for PTX1 (1),¹ it was concluded that ring A in PTX6 (6) contained an equatorial oxygen at C-7. This is reflected in the ROESY data which displayed NOE correlations from H-8 to H-3 as well as to H-5 in 6 (Figure 3). In contrast, these key NOEs were not observed in PTX7 (7), and instead NOEs from H-10 to H-3 as well as to H-41 (Me) were noted (Figure 3). Since the NOE correlations from H-3 to H-4 and H-5 are still observed in 7, it was determined that the oxygen substituent in 7 is axial. Other NOE correlations in ring B (e.g. H-8 to H-9 and H-9 to H-10) supported this assignment and hence PTX7 (7) was identified as the C-7 epimer of 6 (Figure 1). In support of this, the resonances for H-3, H-4_{eq}, and H-5_{ax} in PTX7 (7) were shifted by Δ +0.39, +0.32, and +0.57 ppm, respectively, compared with those of PTX6 (6), consistent with the effect of an axial oxygen substituent on ring A in 7.¹²

The Structure of PTX9 (9). The negative ion FABMS data for PTX9 [m/z : 887 ($\text{M} - \text{H}$)⁻] revealed that the compound was isomeric with PTX6 (6) and PTX7 (7). Once again, in the structural determination work, all NMR measurements were performed with the phenacyl esters in order to compare and contrast with the corresponding NMR data of 6 and 7, as well as prevent the possibility of any spontaneous interconversion. The assignments for PTX9 (9) shown in Table 1, based on the usual series of 1D and 2D spectra, show chemical shift differences for the resonances H-2 through H-13 compared with the corresponding resonances in 6 and 7. In particular, the greatest differences are observed for the protons H-6 through H-11, though paradoxically the two spin systems H-41 (Me) through H-6 and H-8 through H-11 were still present. Whereas the ^1H NMR spectra of 6 and 7 both displayed resonances for all the exchangeable hydroxyl protons (HO-11, HO-36, and HO-37), only the resonances for two hydroxyl signals (HO-36, HO-37) could be accounted for in the spectra of 9. Instead, a new hydroxyl signal (4.61 ppm, broad singlet) was observed, and this was assigned to position 10, based on the correlations appearing in the ^1H - ^1H COSY spectrum. Thus the oxygen at C-11 in 9 must be part of an ether link, arising through expansion of ring B to a tetrahy-

(11) For a detailed review of spiroketal chemistry: Perron, F.; Albizzati, K. F. *Chem. Rev.* **1989**, *89*, 1617.

(12) Satake, M.; Ishibashi, Y.; Legrand, A. M.; Yasumoto, T. *Biosci. Biotech. Biochem.* **1997**, *60*, 2103.

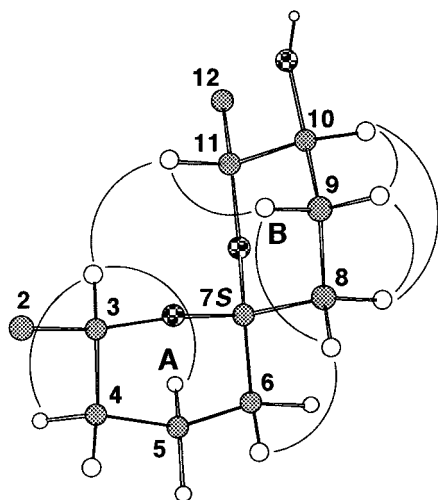


Figure 4. Portions of the PTX8/9 molecules, showing the NOEs around the spiroketal rings A and B.

dropyrans ring and formation of a new spiro[5.5] system. In accord with this proposal, the resonance for C-10 in the ^{13}C NMR spectra of **6** and **7**, which falls in the expected region of 78–85 ppm for carbons comprising a saturated spiro[4.5] system,¹³ experienced a considerable upfield shift (ca 13 ppm) in the spectrum of **9** (Table 1). Further support for structure **9** comes from the magnitude and patterns of coupling for H-10 (ddd, 10, 10 and 4 Hz) and H-11 (d, 10 Hz) which are consistent with their axial configuration. The stereochemistry around C-7 with respect to ring A in **9** was defined by a key NOE between H-3 and H-11 (Figure 4) which indicated that the oxygen at C-7 is axially orientated, and that C-8 is equatorially orientated, as in the case of PTX7 (**7**). Comparison of the NMR data and inspection of the remainder of the NOE data for **9** indicated that there were no differences at the other stereocenters compared with **6** and **7**, and hence the stereochemistry for **9** is as shown (Figure 1).

The Structures of PTX4 (4) and PTX8 (8). The LSI-MS/MS spectra of the $[m/z\ 897\ (\text{M} + \text{Na})^+]$ ion for both PTX1 (**1**) and PTX4 (**4**) were identical, providing further evidence that the molecules were stereoisomers. Since the ^1H NMR spectrum of PTX4 (**4**) showed such a close similarity with that of PTX7 (**7**), it was possible to match many of the crucial assignments for the backbone resonances which greatly facilitated the structural elucidation process (Table 2). In particular, the resonances for C-3, C-4, C-5, C-6, C-7, C-8, C-9, and C-10 were very similar to those of the corresponding resonances in PTX7 (**7**), indicating that the configuration around C-7 was the same in both molecules. On the other hand, the resonances for the same positions in PTX1 (**1**) were similar to the corresponding positions in PTX6 (**6**), supporting a structural relationship between these two congeners. Since the key NOEs which were noted in the PTX6/7 pair were also observed in PTX1/4 (Figure 3), PTX4 (**4**) was identified as 7-*epi*-PTX1 (Figure 1). Extrapolation of the structural correlations between the PTX1/4 and PTX6/7

pairs led to the idea that PTX8 (**8**) possessed the same skeleton as PTX9 (**9**). Once again this was supported by the observation that the 1D and 2D NMR for **8** closely resembled those of **9** (Table 2), and the NOE data as shown in PTX9 (**9**) (Figure 4) confirmed the biaxial orientation of C–O bonds in the spiro[5.5] system in PTX8 (**8**) (Figure 1).

Discussion

To date, only PTX2 (**2**) has been found in extracts of *Dinophysis* cells, and it has been proposed that the PTX congeners **1**, **3**, and **6** are produced through oxidation of the C-43 methyl group of **2** in the digestive gland of the shellfish.³ Following the identification of PTX4 (**4**) and PTX7 (**7**) as the 7-*epi*-derivatives of PTX1 and PTX6, respectively, the question arises as to whether the former pair of congeners are artifacts of the isolation procedure. According to the fluorometric HPLC analytical data using 9-anthryldiazomethane (ADAM) as a fluorescence labeling reagent,¹⁴ the digestive glands of scallops collected from Mutsu Bay, Japan, contained almost equal amounts of PTX6 (5.7 $\mu\text{g/g}$ digestive gland) and PTX7 (5.0 $\mu\text{g/g}$ digestive gland). Although acidic conditions do not prevail during the normal recovery process, a recovery test was performed using digestive glands of nontoxic scallops spiked with PTX6 (57 $\mu\text{g/g}$) and no PTX7 was detected. This indicates that PTX6 (**6**) is stable under these conditions and is not transformed to PTX7 (**7**) during the extraction and analysis procedure. Thus it can be concluded that PTX7 (**7**) and hence PTX4 (**4**) are not artifacts of the extraction process but occur naturally in extracts of scallop digestive glands. Of further significance is the fact that if these compounds were artifacts, it might be expected that PTX8 (**8**) and PTX9 (**9**) would also be observed in the mixture, but careful examination of the fluorometric HPLC data failed to show any evidence of PTX9 in the shellfish extracts.

The occurrence of both epimers of a spiroketal ring system in polyethers such as the pectenotoxin group, is rare. Although a number of dinoflagellate polyether metabolites containing spiroketal rings have been reported,^{4,11} to our knowledge the only other precedent of naturally occurring spiroketal epimers is the recently identified epimers ciguatoxin (CTX) 4A and CTX4B from *Gambierdiscus toxicus*.¹² However, from a consideration of the factors affecting the orientation of the spiro C–O bonds, the occurrence of both spiroketal epimers among the pectenotoxins may not be surprising. In tetrahydropyrans rings the equatorial preference for substituents is important, but other factors including steric effects, anomeric effects, intramolecular hydrogen bonding, and other chelation effects influence this selection.¹¹ From the studies of many spiroketal systems by different groups, it is generally accepted that in spiro[5.5]- and spiro[4.5] systems, the biaxial arrangement of spiro C–O bonds, maximizing the anomeric effect, is favored in compounds containing saturated or unsaturated ether ring systems. Indeed, a biaxial orientation of C–O bonds is found in several marine polyether metabolites including the DSP toxins,⁴ halichondrin,¹⁵ and aplysiatoxin.¹⁶ In contrast to this trend, the X-ray crystallographic evidence for PTX1 (**1**) reveals an equatorial spiro C–O

(13) Relevant examples can be found in: (a) Uemura, D.; Takahashi, K.; Yamamoto, T.; Katayama, C.; Tanaka, J.; Okumura, Y.; Hirata, Y. *J. Am. Chem. Soc.* **1985**, *107*, 4796. (b) Murata, M.; Legrand, A. M.; Scheuer, P. J.; Yasumoto, T. *Tetrahedron Lett.* **1992**, *33*, 525. (c) Pettit, G. R.; Ichihara, Y.; Wurzel, G.; Williams, M. D.; Schmidt, J. M.; Chapuis, J. *J. Chem. Soc., Chem. Commun.* **1995**, 383.

(14) Lee, J.-S.; Yanagi, T.; Kenma, R.; Yasumoto, T. *Agric. Biol. Chem.* **1987**, *51*, 877.

bond in the spiroketal arrangement of rings A and B, and presumably other factors including the conformational restraints of the macrocyclic lactone ring exert an influence over the spiroketal configuration at C-7.¹ Acid treatment of PTX6 (**6**), which contains the same equatorial spiro C–O bond as found in **1**, results in spiroisomerization at C-7 leading to formation of PTX7 (**7**) which possesses a biaxial arrangement of C–O bonds. Interestingly, the isomer PTX9 (**9**) formed concomitantly during this process, also contains the more common biaxial conformation of spiro C–O bonds in the expanded 1,7-dioxo[5.5]undecane system.

It is likely that the spiroisomerization occurs within the digestive gland of the scallop, perhaps selectively mediated by a scallop-derived enzyme as opposed to a random acid-catalyzed process, since the additional 1,7-dioxo[5.5]undecane derivatives (e.g. PTX8 and PTX9) are not observed in the scallop extracts. Other explanations based on biogenetic considerations are less plausible: A putative linear polyketide chain could form the substrate for two different cyclases, which differ only in the stereochemistry of formation of the ring A/B spiroketal system. However, if this were the case, it would be expected that both epimers would be observed in the toxin-producing dinoflagellate.

From the perturbation of the ¹H shifts in other parts of the macrocyclic lactone (see Table 1), and from simple modeling experiments, it is clear that spiroisomerization at C-7 in **4** and **7** affects the overall conformation of the macrocyclic lactone ring, as does expansion to form the spiro[5.5] system. Not surprisingly perhaps, these changes also affect the toxicity of these PTX derivatives in the mouse bioassay. The lethal toxicity of PTX4 was 770 μg/kg (mouse, i.p.),³ which is approximately one-third that of PTX1, while that of PTX7 was more than 5 mg/kg (mouse, i.p.). The toxicities of PTX8 and PTX9 were also diminished, at more than 5 mg/kg (mouse, i.p.). Interestingly, acid treatment of homohalichondrin B, a sponge polyether, caused epimerization at the central spiroketal carbon resulting in significant conformational changes and concomitant changes in cytotoxicity.¹⁷

Conclusion

Both PTX6 (**6**) and PTX7 (**7**) undergo autocatalyzed equilibration, and the process is accelerated by the addition of TFA, whereupon a new derivative PTX9 (**9**) is also produced. Detailed analyses of the NMR data indicated that **7** is the 7-*epi*-derivative of **6** and contains the anomericly favorable biaxial arrangement of C–O bonds at the C-7 spiroketal position. The third product PTX9 (**9**), which is formed concomitantly, arises by opening of the spiro[4.5] system and recyclization to form an enlarged spiro[5.5] system. In an identical manner, PTX1 (**1**) and PTX4 (**4**) undergo equilibration upon treatment with TFA, and **4** was identified as the 7-*epi*-derivative of **1**. An additional third product PTX8 (**8**) was

shown to share the same skeleton as PTX9 (**9**), including the spiro[5.5] system.

Experimental Section

General Methods. All solvents were HPLC grade unless otherwise stated. The ¹H NMR spectra were measured at 400 or 500 MHz or 600 MHz, and the ¹³C NMR spectra were recorded at 100 or 150 MHz. NMR samples were dissolved in C₅D₅N. FAB mass spectra were obtained using 3-nitrobenzyl alcohol as matrix. PTXs were extracted from the digestive glands of DSP-contaminated scallops, *Patinopecten yessoensis*, collected in 1988, from Mutsu Bay, Japan, and were purified and isolated following the previously reported procedures.³ To avoid any interconversion catalyzed by the C-18 carboxyl group, measurements of chemical properties of the PTX6/7/9 congeners were carried out using the corresponding phenacyl ester derivatives.

PTX4 (4): white amorphous solid; [α]²⁰_D +2.07 (*c* 0.193, MeOH); UV_{max} 235 nm (ϵ 12000, MeOH); IR (KBr) 3500, 1760, 1730 cm⁻¹; ¹H and ¹³C NMR data are shown in Table 2.

PTX6 (6) phenacyl ester: white amorphous solid; [α]²⁰_D +8.77 (*c* 0.114, MeOH); UV_{max} 237 nm (ϵ 37000, MeOH); IR (KBr) 3500, 1760, 1730, 1720, 1700 cm⁻¹; ¹H and ¹³C NMR data are shown in Table 1.

PTX7 (7) phenacyl ester: white amorphous solid; [α]²⁰_D +11.5 (*c* 0.131, MeOH); UV_{max} 237 nm (ϵ 37000, MeOH); IR (KBr) 3500, 1760, 1730, 1720, 1700 cm⁻¹; ¹H and ¹³C NMR data are shown in Table 1.

PTX8 (8): white amorphous solid; [α]²⁰_D +19.8 (*c* 0.126, MeOH); UV_{max} 237 nm (ϵ 12000, MeOH); IR (KBr) 3500, 1760, 1730 cm⁻¹; ¹H and ¹³C NMR data are shown in Table 2.

PTX9 (9) phenacyl ester: white amorphous solid; [α]²⁰_D +15.2 (*c* 0.105, MeOH); UV_{max} 239 nm (ϵ 37000, MeOH); IR (KBr) 3500, 1750, 1730, 1720, 1700 cm⁻¹; ¹H and ¹³C NMR data are shown in Table 1.

Preparation of Phenacyl Esters. In a typical procedure, a solution of PTX7 (**7**) (7.1 μmol, 6.3 mg) in acetone (200 μL) containing triethylamine (36 μmol, 5 μL) was treated with phenacyl bromide (15 μmol, 3 mg) at 40 °C for 2 h. The resulting ester was isolated using an ODS column (Cosmosil 5C18-AR, 10 mm × 250 mm; Nacalai Tesque, Kyoto, Japan) and elution with 80% MeCN/H₂O, flow rate 2 mL/min. PTX7 phenacyl ester eluted at *rt* 14.5 min (3.5 mg, yield 49%); LSIMS 1029 (M + Na)⁺. The phenacyl ester of PTX6 prepared in the same way, eluted at *rt* 10.5 min (7.2 mg, yield 64%); LSIMS *m/z* 1029 (M + Na)⁺.

Acid-Catalyzed Rearrangements. In a typical experiment, the phenacyl ester of PTX7 (20 μg) was dissolved in 90% MeCN/H₂O (40 μL) containing 0.1% TFA (v/v) at room temperature. Reaction progress was monitored by LC–UV (Cosmosil 5C18-AR, 4.6 mm × 250 mm; eluant 70% MeCN/H₂O, flow rate 1 mL/min; detection at 235 nm). Under these conditions the order of elution was PTX6 ester (*rt* 7.5 min), PTX7 ester (*rt* 11.0 min) and PTX9 ester (*rt* 15.5 min).

Large Scale Preparation of PTX8 (8) and PTX9 (9). These compounds were obtained by acid treatment of **1** and **6**, respectively, following the reaction conditions described above. The products were purified by HPLC (Cosmosil 5C18-AR, 10 mm × 250 mm; 70% MeCN/H₂O for **8**, 80% MeCN/H₂O supplemented with 0.1% (v/v) acetic acid for **9** as eluant). PTX8 (**8**) was obtained in 29% yield from PTX1 (**1**) and PTX9 (**9**) 35% yield from PTX6 (**6**).

Acknowledgment. We are grateful to Dr. L. Glendenning for his assistance during preparation of this manuscript, to Dr. J. Curtis for recording some of the LSIMS data, and to Mr. H. Onodera for NMR measurements of the PTX1/4/8 congeners. Participation of the second author (J.L.C.W.) in this study was supported by a scholarship from the Japanese Society for Promotion of Science. This work was supported by a grant-in-aid from the Ministry of Education, Science, Sports, and Culture, Japan (NO. 07102002).

JO971310B

(15) (a) Uemura, D.; Takahashi, K.; Yamamoto, T.; Katayama, C.; Tanaka, J.; Okumura, Y.; Hirata, Y. *J. Am. Chem. Soc.* **1985**, *107*, 4796. (b) Pettit, G. R.; Tan, R.; Gao, F.; Williams, M. D.; Doubek, D. L.; Boyd, M. R.; Schmidt, J. M.; Chapuis, J.-C.; Hamel, E.; Bai, R.; Hooper, J. N. A.; Tackett, L. P. *J. Org. Chem.* **1993**, *58*, 2538. (c) Litaudon, M.; Hart, J. B.; Blunt, J. W.; Lake, R. J.; Munro, M. H. G. *Tetrahedron Lett.* **1994**, *35*, 9435.

(16) Moore, R. E.; Blackman, A. J.; Cheuk, C. E.; Mynderse, J. S.; Matsumoto, G. K.; Clardy, J.; Woodard, R. W.; Craig, J. C. *J. Org. Chem.* **1984**, *49*, 2484.

(17) Hart, J. B.; Blunt, J. W.; Munro, M. H. G. *J. Org. Chem.* **1996**, *61*, 2888.